MODELLING OF PULSATING DIFFUSIONAL BOUNDARY LAYERS—II A REVERSIBLE REDOX ELECTROCHEMICAL REACTION INVOLVING SOLUBLE SPECIES IN SOLUTION THEORY AND EXPERIMENTAL TEST

C I ELSNER, C L PERDRIEL, S L MARCHIANO and A J ARVIA

Instituto de Investigaciones Fisicoquimicas Teoricas y Aplicadas (INIFTA) Facultad de Ciencias Exactas, Universidad Nacional de La Plata Sucursal 4, Casilla de Correo 16, (1900) La Plata, Argentina

Abstract—A solution of the diffusion equation for a reversible redox electrochemical reaction in the presence of only one species (the reactant) and in the absence of products at the initiation of the reaction for a square wave perturbing potential is presented The solution furnishes the concentration profiles for reactant and product and their dependence on the time elapsed from the initiation of the halfcycle t', on the frequency of the periodic potential, on the number of cycles, N, and on the symmetry of the signal In addition, the dependences of the current on t' and N, and that of the charge density on N, were obtained Conclusions from the theory are experimentally verified by using the reversible $[Fe(CN)_6]^{4-}/[Fe(CN)_6]^{3-}$ redox couple on platinum as a test reaction

1. INTRODUCTION

The application of periodic perturbing potentials to electrodes in contact with electrolyte solutions produces different changes at the interphase depending on the potential limits (E_a and E_c), frequency (f) and time-symmetry of the perturbation[1–5] For a simple electrochemical reaction involving soluble species in solution, these changes can be assigned to modifications of charging of the electrical double layer (non-faradaic process) and variation of local concentrations of reactant and product in the vicinity of the electrode caused by the faradaic process For the sake of simplicity, one can consider as a first approach that the relative contribution of non-faradaic to faradaic processes is negligible When the faradaic process proceeds by applying a periodic perturbing potential and occurs under either diffusion or intermediate kinetics control, concentration gradients at the electrode–solution interphase are established Correspondingly, pulsating diffusion boundary layers are built up for the concentrations of reactant and product involved in both the anodic and cathodic reactions, respectively The general behaviour of each one of these layers for a fixed geometry depends on the properties of the solution, kinetic parameters of the electrochemical reaction and perturbing potential conditions Thus, for a particular electrochemical reaction subjected to a time-symmetric square wave perturbing potential, which is potential-symmetric with respect to its equilibrium potential, the average thicknesses of the diffusion boundary layers for a constant number of cycles decrease as f increases[5]

As far as the entire kinetics of the electrochemical reaction is concerned, the frequency dependence of the diffusion boundary layer thickness brings about various important consequences Firstly, the fact that, in principle, a frequency, f_t, should be found at which one can observe a transition in the kinetics of the reaction from a mass transport control, for $f < f_t$, to an activation control, for $f > f_t$ This transition depends on the $[k_f/D_{ox}^{1/2} + k_b/D_{re}^{1/2}]$ term[6, 7], where k_f and k_b are the kinetic constants for the forward and backward reactions, respectively, and D_{re} and D_{ox} denote the diffusion coefficients of species entering the anodic and cathodic reactions, respectively Details about the kinetic transition deserves an extensive discussion in a forthcoming publication[8] Secondly, it should be noticed that the validity of the electroneutrality condition should depend on the rate of mass transport and frequency of the periodic perturbing potential Thus, in dealing with a fast electrochemical reaction at low values of f, the thickness of the diffusion boundary layers become sufficiently large to fulfill the electroneutrality requirement for solving the pure diffusion problem as expressed throughout Fick's equations[7] However, a more complex situation arises at large values of f, ie small thickness of the diffusion boundary layer and diluted electrolyte solution where an increasing departure from the above mentioned condition should be expected[9]

The present work is devoted to solve the diffusion equation for a fast redox electrochemical reaction produced by means of a square wave perturbing potential in the absence of products at the initiation of the reaction The theoretical approach considers that non-faradaic processes are negligible, that the electroneutrality condition at the diffusion boundary layer is satisfied and, correspondingly, that there is no migration contribution term Furthermore, the redox electrochemical process behaves as an ideal reversible reaction, ie it implies a large exchange current density value In this way the model allows to explicit the concentration profiles for reactant and product the influence of f and the number of cycles, N, as well as the influence of the symmetry of the perturbing poten-

tial Conclusions from the theory are experimentally verified by studying an electrochemical test reaction in a suitable cell design These results are relevant to deal with the more complex situations precedingly described

2. SOLUTION OF THE DIFFUSION EQUATION

Let us consider a fast electrode reaction involving soluble species in solution represented by the equation

$$ox + e^- = re,\qquad (1)$$

which takes place under diffusion control at an inert solid semi-infinite *plane* electrode The oxidized and reduced states of the species in solution are denoted as ox and re respectively For the selected electrode geometry, the concentration profiles of ox and re at any instant, can be obtained by solving Fick's equation for each species in the x-direction, the latter being chosen perpendicular to the electrode surface

$$\frac{\partial c_{ox}(x, t)}{\partial t} = D_{ox}\frac{\partial^2 c_{ox}(x, t)}{\partial x^2},$$

and   (2)

$$\frac{\partial c_{re}(x, t)}{\partial t} = D_{re}\frac{\partial^2 c_{re}(x, t)}{\partial x^2},$$

where the c_{ox} and c_{re} refer to the concentrations of ox and re, respectively, and D_{ox} and D_{re}, the corresponding diffusion coefficients which are assumed to be ct' independent values

2 1 *The general case*

Reaction (1) proceeds under a square wave perturbing potential, ie successive cathodic, E_c, and anodic, E_a, potential steps The frequency of the perturbing potential is $f = 1/T = 1/(\tau_a + \tau_c)$, where T is the period, and τ_a and τ_c are the anodic and cathodic halfperiods, respectively The values of E_a and E_c are set in such a way that $E_a > E_r^\circ$ and $E_c < E_r^\circ$, E_r° denoting the standard potential of redox reaction (1)

To solve Fick's equations the following initial and boundary conditions are considered For $t = 0$,

$$\left.\begin{array}{c}c_{ox} = c^0\\c_{re} = 0\end{array}\right\},\qquad (3)$$

and for $t > 0$ and $x = 0$

$$\frac{c_{ox}(0, t)}{c_{re}(0, t)} = \theta = \exp\left[\frac{zF}{RT}(E_c - E_r^0)\right],$$

for odd halfcycles,   (4a)

$$\frac{c_{ox}(0, t)}{c_{re}(0, t)} = \psi = \exp\left[\frac{zF}{RT}(E_a - E_r^0)\right],$$

for even halfcycles,   (4b)

and

$$D_{ox}\left(\frac{\partial c_{ox}(x, t)}{\partial x}\right)_{x=0} + D_{re}\left(\frac{\partial c_{re}(x, t)}{\partial x}\right)_{x=0} = 0,\qquad (5)$$

where the time t, is defined as follows

$$t = ((N-1)/2)(\tau_a + \tau_c) + t',\quad \text{for odd values of } N$$

and

$$t = (N/2)\tau_c + (N/2 - 1)\tau_a + t',\quad \text{for even values of } N,$$

where

$$0 < t' < \tau_c,\quad \text{for odd values of } N,$$

$$0 < t' < \tau_a,\quad \text{for even values of } N,$$

and N represents the total number of halfcycles For $N = 1$, the first cathodic halfcycle, the concentration profiles for ox and re are given by the well-known equations given elsewhere[7]

The general solution of Fick's equations for any value of N for the cathodic and the anodic halfcycles respectively, are given by the following expressions For odd values of N

$$\frac{c_{ox}(x, t)}{c^0} = \frac{1}{1+\gamma^{1/2}\theta}$$

$$\times\left[\gamma^{1/2}\theta + \sum_{k=1}^{(N+1)/2}\text{erf}\frac{x}{2\sqrt{D_{ox}}\sqrt{A+t'}}\right.$$

$$\left.-\sum_{k=0}^{(N-2)/2}\text{erf}\frac{x}{2\sqrt{D_{ox}}\sqrt{B+t'}}\right]$$

$$+\frac{1}{1+\gamma^{1/2}\psi}\left[\sum_{k^*=1}^{(N-1)/2}\text{erf}\frac{x}{2\sqrt{D_{ox}}\sqrt{E+t'}}\right.$$

$$\left.-\sum_{k=0}^{(N-2)/2}\text{erf}\frac{x}{2\sqrt{D_{ox}}\sqrt{P+t'}}\right],\qquad (6)$$

and

$$\frac{c_{re}(x, t)}{c^0} = \frac{\gamma^{1/2}}{1+\gamma^{1/2}\theta}\left[1 + \sum_{k=0}^{(N-2)/2}\text{erf}\frac{x}{2\sqrt{D_{re}}\sqrt{B+t'}}\right.$$

$$\left.-\sum_{k=1}^{(N+1)/2}\text{erf}\frac{x}{2\sqrt{D_{re}}\sqrt{A+t'}}\right]+\frac{\gamma^{1/2}}{1+\gamma^{1/2}\psi}$$

$$\times\left[\sum_{k=0}^{(N-2)/2}\text{erf}\frac{x}{2\sqrt{D_{re}}\sqrt{P+t'}}\right.$$

$$\left.-\sum_{k^*=1}^{(N-1)/2}\text{erf}\frac{x}{2\sqrt{D_{re}}\sqrt{E+t'}}\right],\qquad (7)$$

and for even values of N

$$\frac{c_{ox}(x, t)}{c^0} = \frac{1}{1+\gamma^{1/2}\theta}\left[\sum_{k=0}^{(N-2)/2}\text{erf}\frac{x}{2\sqrt{D_{ox}}\sqrt{G+t'}}\right.$$

$$\left.-\sum_{k=1}^{(N+1)/2}\text{erf}\frac{x}{2\sqrt{D_{ox}}\sqrt{A+t'}}\right]+\frac{1}{1+\gamma^{1/2}\psi}$$

$$\times\left[\gamma^{1/2}\psi + \sum_{k=0}^{(N-2)/2}\text{erf}\frac{x}{2\sqrt{D_{ox}}\sqrt{P+t'}}\right.$$

$$\left.-\sum_{k^*=1}^{(N-1)/2}\text{erf}\frac{x}{2\sqrt{D_{ox}}\sqrt{S+t'}}\right],\qquad (8)$$

and

$$\frac{c_{re}(x, t)}{c^0} = \frac{\gamma^{1/2}}{1+\gamma^{1/2}\theta}\left[\sum_{k=1}^{(N+1)/2}\operatorname{erf}\frac{x}{2\sqrt{D_{re}}\sqrt{A+t'}}\right.$$

$$-\sum_{k=0}^{(N-2)/2}\operatorname{erf}\frac{x}{2\sqrt{D_{re}}\sqrt{G+t'}}\right]$$

$$+\frac{\gamma^{1/2}}{1+\gamma^{1/2}\psi}\left[1+\sum_{k^*=1}^{(N-1)/2}\operatorname{erf}\frac{x}{2\sqrt{D_{re}}\sqrt{S+t'}}\right.$$

$$\left.-\sum_{k=0}^{(N-2)/2}\operatorname{erf}\frac{x}{2\sqrt{D_{re}}\sqrt{P+t'}}\right], \tag{9}$$

being $k'=(k+1)/2$, $k''=(k-2)/2$, $k^*=(k-1)/2$ where $1\leq k\leq N$, and $\gamma=D_{ox}/D_{re}$

To simplify the expressions it has been considered that

$$A=(k'-1)(\tau_a+\tau_c), \quad B=(k''+1)\tau_a+k''\tau_c,$$

$$E=k^*\tau_a+(k^*-1)\tau_c, \quad P=k''(\tau_a+\tau_c),$$

$$G=(k''+1)\tau_c+k''\tau_a, \quad S=k^*\tau_c+(k^*-1)\tau_a$$

From the concentration profiles of c_{ox} and c_{re} for odd and even values of N, equations (6) and (9), the fluxes of the reactants involved in the cathodic and anodic reactions expressed as current densities, j_c and j_a, respectively, can be immediately obtained For the cathodic current density

$$j_c = -zFD_{ox}\left(\frac{\partial c_{ox}(x, t)}{\partial x}\right)_{x=0}$$

$$= -\frac{zFD_{ox}^{1/2}c^0}{\sqrt{\pi}}\left[\frac{1}{1+\gamma^{1/2}\theta}\left(\sum_{k=1}^{(N+1)/2}\frac{1}{\sqrt{A+t'}}\right.\right.$$

$$\left.-\sum_{k=0}^{(N-2)/2}\frac{1}{\sqrt{B+t'}}\right)+\frac{1}{1+\gamma^{1/2}\psi}\left(\sum_{k^*=1}^{(N-1)/2}\frac{1}{\sqrt{E+t'}}\right.$$

$$\left.\left.-\sum_{k=0}^{(N-2)/2}\frac{1}{\sqrt{P+t'}}\right)\right], \tag{10}$$

and for the anodic current density

$$j_a = zFD_{re}\left(\frac{\partial c_{re}(x, t)}{\partial x}\right)_{x=0}$$

$$= \frac{zFD_{ox}^{1/2}c^0}{\sqrt{\pi}}\left[\frac{1}{1+\gamma^{1/2}\theta}\left(\sum_{k=1}^{(N-1)/2}\frac{1}{\sqrt{A+t'}}\right.\right.$$

$$\left.-\sum_{k=0}^{(N-2)/2}\frac{1}{\sqrt{G+t'}}\right)+\frac{1}{1+\gamma^{1/2}\psi}\left(\sum_{k^*=1}^{(N-1)/2}\frac{1}{\sqrt{S+t'}}\right.$$

$$\left.\left.-\sum_{k=0}^{(N-2)/2}\frac{1}{\sqrt{P+t'}}\right)\right] \tag{11}$$

On the other hand, the cathodic and anodic charge densities, q_c and q_a, comprised in each halfcycle, result from the integration of equations (10) and (11) respect-

ively Thus, it results

$$q_c = \int_0^{\tau_c} j_c\, dt$$

$$= -\frac{zFD_{ox}^{1/2}c^0}{\sqrt{\pi}}\left[\frac{2}{1+\gamma^{1/2}\theta}\left(\sum_{k=1}^{(N+1)/2}\sqrt{H}\right.\right.$$

$$\left.-\sum_{k=1}^{(N+1)/2}\sqrt{A}+\sum_{k=0}^{(N-2)/2}\sqrt{B}-\sum_{k=0}^{(N-2)/2}\sqrt{L}\right)$$

$$+\frac{2}{1+\gamma^{1/2}\psi}\left(\sum_{k=0}^{(N-2)/2}\sqrt{P}-\sum_{k=0}^{(N-2)/2}\sqrt{G}\right.$$

$$\left.\left.+\sum_{k^*=1}^{(N-1)/2}\sqrt{M}-\sum_{k^*=1}^{(N-1)/2}\sqrt{E}\right)\right], \tag{12}$$

and

$$q_a = \int_0^{\tau_a} j_a\, dt$$

$$= \frac{zFD_{ox}^{1/2}c^0}{\sqrt{\pi}}\left[\frac{2}{1+\gamma^{1/2}\theta}\left(\sum_{k=1}^{(N+1)/2}\sqrt{U}\right.\right.$$

$$\left.-\sum_{k=1}^{(N+1)/2}\sqrt{A}+\sum_{k=0}^{(N-2)/2}\sqrt{G}-\sum_{k=0}^{(N-2)/2}\sqrt{L}\right)$$

$$+\frac{2}{1+\gamma^{1/2}\psi}\left(\sum_{k=0}^{(N-2)/2}\sqrt{P}-\sum_{k=0}^{(N-2)/2}\sqrt{B}\right.$$

$$\left.\left.+\sum_{k^*=1}^{(N-1)/2}\sqrt{M}-\sum_{k^*=1}^{(N-1)/2}\sqrt{S}\right)\right], \tag{13}$$

where $H=k'\tau_c+(k'-1)\tau_a$, $L=(k''+1)(\tau_a+\tau_c)$, $M=k^*(\tau_a+\tau_c)$, $U=k'\tau_a+(k'-1)\tau_c$

2 2 The case of time-symmetric perturbation $(\tau_c=\tau_a)$

Let us consider the particular situation when $\tau_c=\tau_a=\tau$, ie a time-symmetric perturbing potential is applied to the electrode In this case from the generalized concentration profiles given by equations (6) to (9) one obtains for odd values of N

$$\frac{c_{ox}(x, t)}{c^0} = \frac{1}{1+\gamma^{1/2}\theta}\left[\gamma^{1/2}\theta+\sum_{k=1}^{N}(-1)^{k+1}\right.$$

$$\left.\operatorname{erf}\frac{x}{2\sqrt{D_{ox}}\sqrt{(k-1)\tau+t'}}\right]+\frac{1}{1+\gamma^{1/2}\psi}$$

$$\left[\sum_{k=2}^{N}(-1)^{k+1}\operatorname{erf}\frac{x}{2\sqrt{D_{ox}}\sqrt{(k-2)\tau+t'}}\right], \tag{14}$$

$$\frac{c_{re}(x, t)}{c^0} = \frac{\gamma^{1/2}}{1+\gamma^{1/2}\theta}\left[1+\sum_{k=1}^{N}\right.$$

$$\left.(-1)^k\operatorname{erf}\frac{x}{2\sqrt{D_{re}}\sqrt{(k-1)\tau+t'}}\right]$$

$$+\frac{\gamma^{1/2}}{1+\gamma^{1/2}\psi}\left[\sum_{k=2}^{N}(-1)^k\operatorname{erf}\frac{x}{2\sqrt{D_{re}}\sqrt{(k-2)\tau+t'}}\right], \tag{15}$$

and for even values of N

$$\frac{c_{ox}(x, t)}{c^0} =$$

$$\frac{1}{1+\gamma^{1/2}\theta} \left[\sum_{k=1}^{N} (-1)^k \, \text{erf} \frac{x}{2\sqrt{D_{ox}} \sqrt{(k-1)\tau+t'}} \right]$$

$$+\frac{1}{1+\gamma^{1/2}\psi} \left[\gamma^{1/2}\psi + \sum_{k=2}^{N} (-1)^k \right.$$

$$\text{erf} \frac{x}{2\sqrt{D_{ox}} \sqrt{(k-2)\tau+t'}} \left. \right], \qquad (16)$$

$$\frac{c_{re}(x, t)}{c^0} = \frac{\gamma^{1/2}}{1+\gamma^{1/2}\theta} \left[\sum_{k=1}^{N} (-1)^{k+1} \right.$$

$$\text{erf} \frac{x}{2\sqrt{D_{re}} \sqrt{(k-1)\tau+t'}} \left. \right] + \frac{\gamma^{1/2}}{1+\gamma^{1/2}\psi}$$

$$\left[1 + \sum_{k=2}^{N} (-1)^{k+1} \, \text{erf} \frac{x}{2\sqrt{D_{re}} \sqrt{(k-2)\tau+t'}} \right] \qquad (17)$$

From equations (14) and (17) results

$$J_{a,c} =$$

$$\pm \frac{zFc^0 D_{ox}^{1/2}}{\sqrt{\pi}} \left[\frac{1}{1+\gamma^{1/2}\theta} \sum_{k=1}^{N} (-1)^{k+1} \right.$$

$$\frac{1}{\sqrt{(k-1)\tau+t'}}$$

$$+\frac{1}{1+\gamma^{1/2}\psi} \sum_{k=2}^{N} (-1)^{k+1} \frac{1}{\sqrt{(k-2)\tau+t'}} \left. \right], \qquad (18)$$

and by integration to cover the time range τ, the charge density equation is accomplished

$$q_{a\,c} = \pm \frac{zFD_{ox}^{1/2}c^0}{\sqrt{\pi}} \left[\frac{4}{1+\gamma^{1/2}\theta} \right.$$

$$\left((-1)^{k+1} \sum_{k=1}^{N-1} \sqrt{k\tau} + \frac{(-1)^{k+1}}{2} \sqrt{k\tau} \right)$$

$$+\frac{4}{1+\gamma^{1/2}\psi} \left((-1)^{k+1} \sum_{k=1}^{N-2} \sqrt{k\tau} \right.$$

$$\left. +\frac{(-1)^{k-1}}{2} \sqrt{(k-1)\tau} \right) \left. \right] \qquad (19)$$

The analysis of these equations and the corresponding experimental test are given in the following sections

3. CONCLUSIONS FROM THE THEORETICAL EQUATIONS

3 1 *The case* $\tau_c > \tau_a$

The equations determining the concentration profiles for ox and re can be plotted in a dimensionless form as $c_{ox}(x, t)/c^0$ and $c_{re}(x, t)/c^0$ *vs* X^*, where

$X^* = 10X/X_{max}$ and $X_{max} = 4\sqrt{D_{ox}\tau_c}$ This type of plot is depicted in Fig 1 for $\tau_c = 10^{-1}$ s, $\tau_a = 10^{-3}$ s and $\Delta E = |E_c - E_r^0| = |E_a - E_r^0| = 0\,2$ V

The concentration profiles of ox and re which are built up during the first cathodic halfcycle, ie $N=1$ and τ_c (Fig 1a), are similar to those earlier described in the literature[7] for reaction (1) under a potential step In the first halfcycle, as the time of application of the potential perturbation increases, the thickness of the diffusion boundary layer also increases for both ox and re But a more complex situation arises for the subsequent halfcycles Hence, for each cathodic halfcycle, and a present value of X^*, the concentration of ox decreases as t' increases The reverse effect is noticed for the concentration of re Furthermore, for even values of N, ie anodic halfcycles, (Figs 1b and d) both concentration profiles exhibit for a certain value of X^* a change in the sign of the derivative, corresponding to a minimum value of $c_{ox}(x, t)/c^0$ and to a maximum value of $c_{re}(x, t)/c^0$ For both species the bulk concentration is asymptotically attained as X^* increases The values of X^* where the minimum value of the dimensionless concentration of ox, and the maximum value of the dimensionless concentration of re are found, increase according to the value of t' for each halfcycle

Nevertheless, as the number of reduction–oxidation halfcycles increased the differences in the concentration profiles for different values of t' are progressively smaller, finally attaining concentration profiles which exhibit only modifications for small values of X^* (Figs 1c and d)

Otherwise, when $\tau_c/\tau_a \gg 1$, as far as the development of the concentration profiles is concerned, the influence of the anodic halfcycle on the subsequent cathodic halfcycle becomes negligible, and the development of the ox concentration profile occurs nearly as if it is due exclusively to the cathodic step applied during the time t In contrast, the influence of the cathodic halfcycle on the development of both the concentration profiles of re and ox during the subsequent anodic halfcycle is quite noticeable In the anodic halfcycles one can observe changes in the concentration profiles already for small values of X^* which correspond to an increase in c_{ox} and a decrease in c_{re} as N increases From $X^* = 2$ upwards the concentration profiles tend to coincide with those resulting for the cathodic halfcycles

3 2 *The case* $\tau_a > \tau_c$

When the square wave perturbing potential involves the condition $\tau_a/\tau_c \geqslant 100$, the concentration profiles resulting for re and ox during the cathodic halfcycle are similar to those already known for reaction (1) proceeding under a constant potential step, ie the concentration profile of ox increases monotonously with X^* to approach the bulk solution concentration, whereas the opposite trend results for the concentration profile of re For both cases the diffusion layer becomes thicker as t' increases Furthermore, only a slight change in the concentration profiles with N can be noticed

On the other hand, for the anodic halfcycles the changes of the concentrations of ox and re with X^* and t' as well as with N are very small
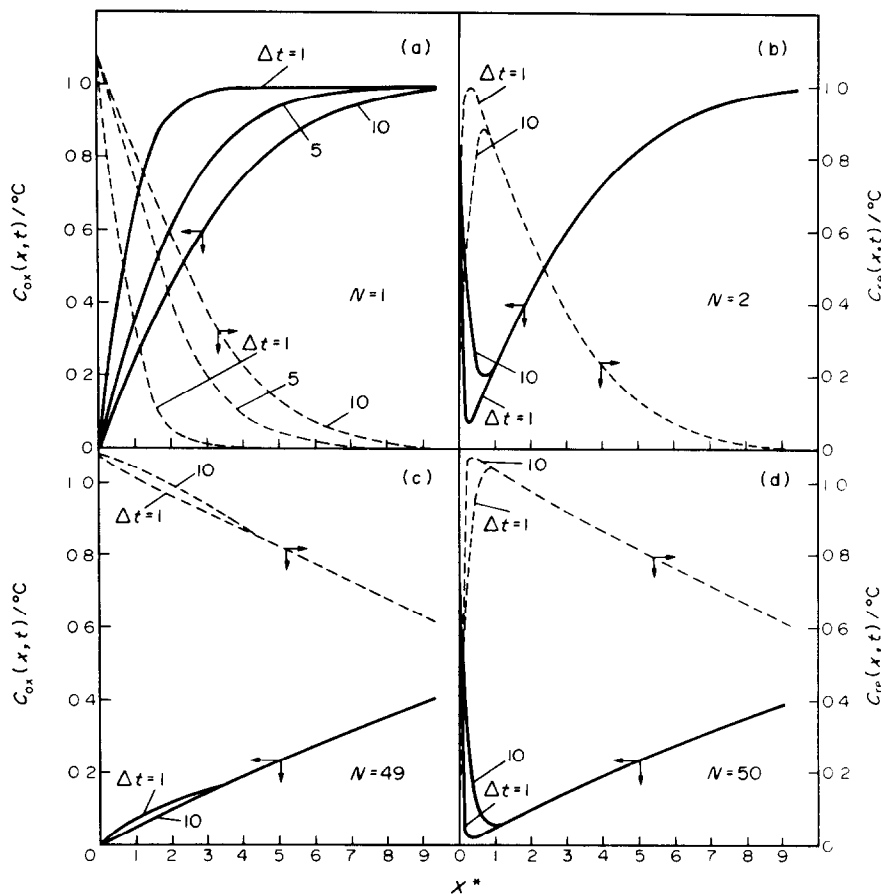
Fig 1 Concentration profiles for ox and re, resulting from the theoretical equation for a time-asymmetric square wave perturbing potential $\tau_a = 10^{-3}$ s, $\tau_c = 0\ 1$ s, $D_{ox} = 6 \times 10^{-6}$ cm^2 s^{-1}, $D_{re} = 5 \times 10^{-6}$ cm^2 s^{-1}, $\Delta E = 0\ 2$ V (a) 1st halfcycle (cathodic), $\Delta t = 10t'/\tau_c$, (b) 2nd halfcycle (anodic), $\Delta t = 10t'/\tau_a$, (c) 49th halfcycle (cathodic), $\Delta t = 10t'/\tau_c$, (d) 50th halfcycle (anodic), $\Delta t = 10t'/\tau_a$

3 3 The symmetric case $\tau_a = \tau_c = \tau$

Comparable conclusions can be derived for reaction (1) proceeding under a symmetric square wave perturbing potential The concentration profiles in this case are plotted by considering $\tau = 1$ s and $|E_c - E_r^0| = |E_a - E_r^0| = 0\ 2$ V (Fig 2) Again a conventional behaviour results for the first cathodic halfcycle ($N = 1$) (Fig 2a) Otherwise, for the first anodic halfcycle ($N = 2$) (Fig 2b) as well as for other even values of N (Fig 2d) one can observe a minimum value of c_{ox} for a certain value of X^*, and as t' increases the minimum value of c_{ox} moves towards greater values of X^* and it tends to smear out Simultaneously, the value of the c_{ox}/c^0 ratio increases according to t' As X^* increases beyond the minimum value, the value of c_{ox} approaches asymptotically the concentration of ox in the bulk

The concentration profiles of ox and re resulting in the following cathodic halfcycles, ie odd values of N, show a maximum value of c_{ox} and a minimum value of c_{re} for small values of t' The values of c_{ox} in the bulk of the solution decrease as N increases In this case one can also observe that the maximal value of c_{ox} and the minimum value of c_{re} tend to disappear as t' increases

It should be noticed that for the symmetric perturbing potential the evolution of the concentration profiles for each halfcycle is largely influenced by the changes produced in the precedent halfcycle

On the other hand, the concentration profiles for c_{re} are nearly the specular image of those already described for c_{ox} (Figs 2a–d)

4. EXPERIMENTAL TEST OF THE THEORETICAL CONCLUSIONS

The conclusions from the theory were verified with data obtained for the following electrochemical reaction

$$[Fe(CN)_6]^{3-} + e^- = [Fe(CN)_6]^{4-}, \qquad (20)$$
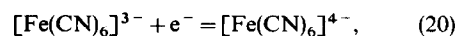
proceeding on a mirror polished platinum electrode under a square wave perturbing potential in the presence of a supporting electrolyte For the purpose of the present work reaction (20) on Pt can be considered as a sufficiently fast, reproducible and clean process under diffusion control
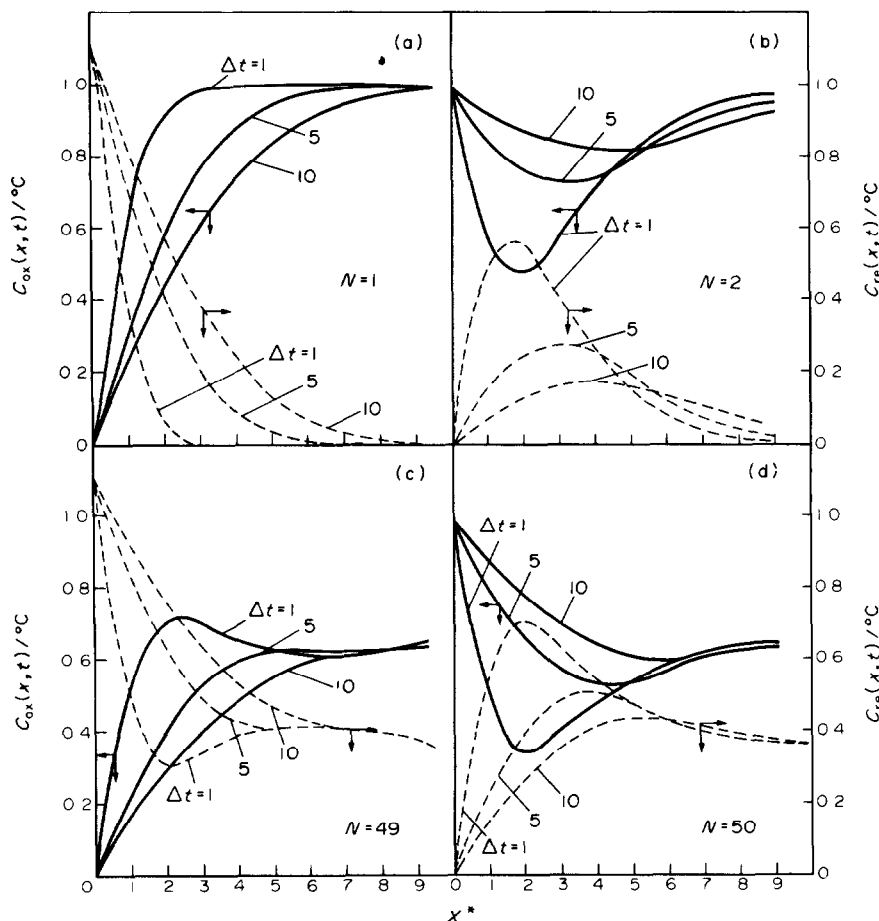
Fig 2 Concentration profiles for ox and re, resulting from the theoretical equation for a time-symmetric square wave perturbing potential $\tau = 1$ s, $D_{ox} = 6 \times 10^{-6}$ cm^2 s^{-1}, $D_{re} = 5 \times 10^{-6}$ cm^2 s^{-1}, $\Delta E = 0\,2$ V, $\Delta t = 10 t'/\tau$ (a) 1st halfcycle (cathodic), (b) 2nd halfcycle (anodic), (c) 49th halfcycle (cathodic), (d) 50th halfcycle (anodic)

4 1 *Experimental*

The electrochemical runs were performed in a single compartment Pyrex glass cell of about 200 cm^3 capacity The working electrode consisted of a Pt sheet of 0 096 cm^2 geometric area mounted into a glass piece The counter electrode was also made from a Pt sheet, its geometric area was 4 cm^2, and it was arranged parallel with respect to the working electrode a distance sufficiently shorter to achieve a primary current distribution as homogeneous as possible A saturated calomel electrode (sce) connected through a capillary tip close to the working electrode and properly shielded to avoid Hg$_2^{2+}$ ion diffusion into the cell was employed as reference The electrolyte solution was prepared from K$_3$[Fe(CN)$_6$], Merck p a, NaOH, Carlo Erba p a, and MilliQ water, and the initial concentration of the reacting species, c^0, was determined through conventional chemical analysis The solution composition used throughout the work was 0 01 M K$_3$[Fe(CN)$_6$] + 1 M NaOH Runs were made at 25°C

The square wave perturbing potential was applied through a fast rise time potentiostat operated by a

square wave generator The current response was recorded through a Nicolet oscilloscope The frequency range of the perturbing potential was 10^4 Hz $\geqslant f \geqslant 5 \times 10^{-2}$ Hz and the value of ΔE was $\pm 0\,2$ V

4 2 *Comparison of experimental results and theoretical predictions*

4 2 1 *Current transients*

Let us first consider that $\tau_c = 0\,1$ s, $\tau_a = 10^{-3}$ s, ie $\tau_a < \tau_c$, and $|E_c - E_r^0| = |E_a - E_r^0| = 0\,2$ V The comparison of the theoretical and experimental data, as shown in Fig 3, is certainly very good The current response for the successive cathodic halfcycles generates an envelope which tends to coincide with that expected for a single potential step with the value of ΔE applied during the time t The cathodic current decreases along the subsequent cathodic halfcycles

On the other hand when $\tau_a > \tau_c$, again a good coincide between theory and experiment is obtained In this case one observes a rapid trend of the cathodic current transient to reach a stationary reproducible
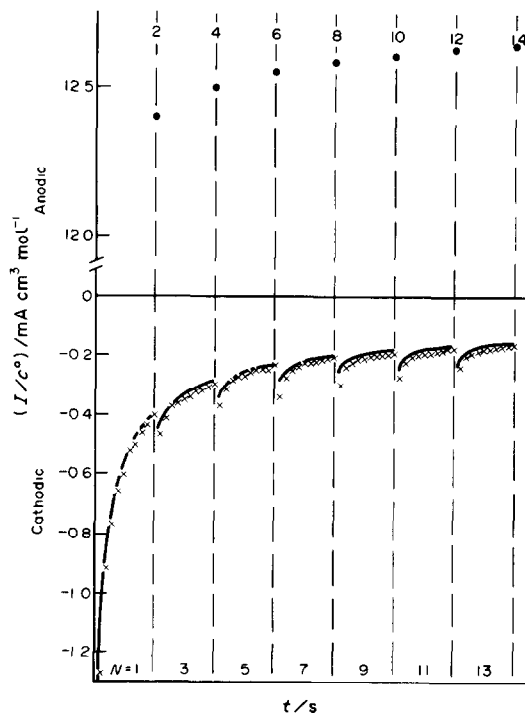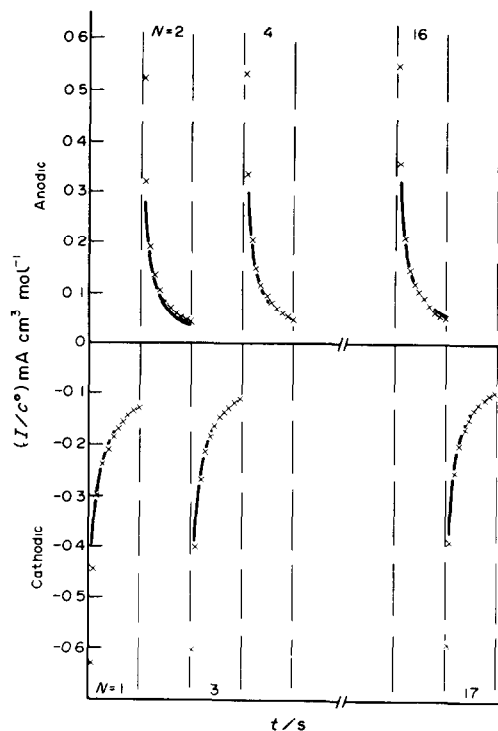
Fig 3 Comparison between theoretical and experimental current transients vs the number of halfcycles for a time-asymmetric square wave perturbing potential $\tau_a = 10^{-3}$ s, $\tau_c = 0\,1$ s, $\Delta E = 0\,2$ V

Fig 4 Comparison between theoretical and experimental current transient vs the number of halfcycles for a time-symmetric square wave perturbing potential $\tau = 1$ s, $\Delta E = 0\,2$ V

situation, which can be related to the fact that the low anodic current values reached, ie 50–100 μA, becomes sufficient to allow the complete disappearance of the small amount of re produced in the preceding cathodic halfcycle

Finally, it is interesting to analyze data for the symmetric case, $\tau_c = \tau_a = \tau$ In this case, both anodic and cathodic current transients obtained for $\tau = 1$ s (Fig 4) decay relatively rapid according to the duration of the halfcycle Nevertheless, in any case, it appears that for a fixed value of t' the current in the anodic halfcycles is always rather smaller than in the cathodic halfcycles

On the other hand, the current in the anodic halfcycles read for $t' = \tau$ tends to increase as N increases, as it should occur according to the concentration profiles (Fig 2) when the concentration of re in solution has been increased Similarly, the current for the cathodic halfcycles diminishes as N increases, as it should be expected for a gradual decrease in ox concentration with t' Once more the agreement between theory and experiment is quite satisfactory Similar results have been also obtained for the three cases in the entire frequency range covered in the present work

4 2 2 *Charge density plots* From equations (12) and (13) it is possible to calculate the amount of product going into solution along the potential cycling This calculation for the case of the asymmetric square wave perturbing potentials is shown in Fig 5 In this case one can observe that for $\tau_a = 10^{-3}$ s,
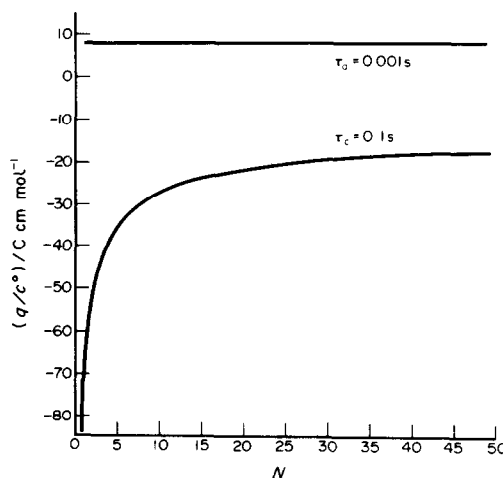

Fig 5 Normalized charge densities (q/c°) for anodic and cathodic halfcycles ιs the number of halfcycles, for a time-asymmetric square wave perturbing potential $\tau_a = 10^{-3}$ s, $\tau_c = 0\,1$ s, $\Delta E = 0\,2$ V

$\tau_c = 0\,1$ s and $\Delta E = 0\,2$ V, the cathodic charge decreases sharply with N, whereas the anodic charge remains practically constant

The charge difference, Δq, accumulated along the successive oxidation–reduction cycles can be immedi-

ately calculated through the following relationship

$$\Delta q = \sum_{k=0}^{N} q_{a}(k'') - \left| \sum_{k=1}^{N} q_{c}(k') \right| \qquad (21)$$

A plot of Δq vs N is illustrated in Fig 6 by using for this case the values of τ_a, τ_c and ΔE referred to above This plot shows an increase in the cathodic charge, ie an increase of the concentration of re in solution, as N is increased Certainly, the value of Δq depends on the number of halfcycles considered and on the frequency of the periodic perturbation

On the other hand, when the same analysis is extended to the symmetric case, ie $\tau_a = \tau_c = \tau$, for $\tau = 1$ s and $\Delta E = 0\,2$ V (Fig 7), the charge accumulated per anodic halfcycle increases according to N, but, the opposite effect is observed for the cathodic halfcycle For the latter the change of q with N for the symmetric case is much smoother than that already described for the asymmetric one The Δq vs N plots for the symmetric case (Fig 8) show qualitatively the same behaviour already described for the Δq vs N plots for the asymmetric case
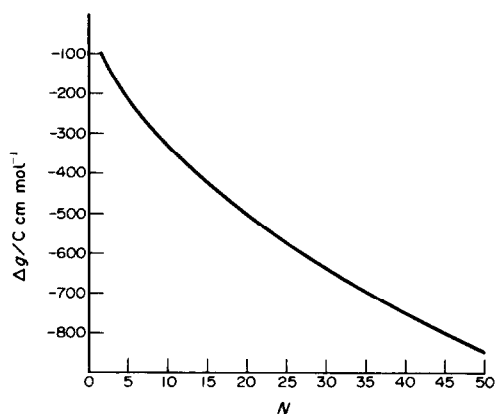

Fig 6 Plot of Δq vs the number of halfcycles, for a time-asymmetric square wave perturbing potential $\tau_a = 10^{-3}$ s, $\tau_c = 0\,1$ s, $\Delta E = 0\,2$ V
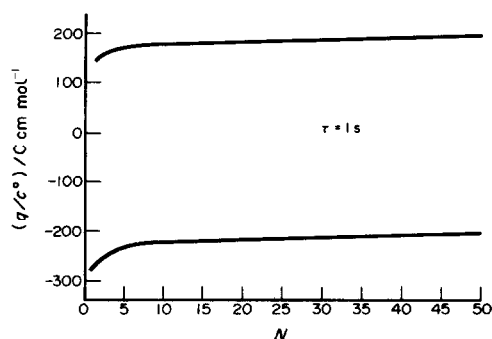

Fig 7 Normalized charge densities (q/c°) for anodic and cathodic halfcycles vs the number of halfcycles, for a time-symmetric square wave perturbing potential $\tau = 1$ s, $\Delta E = 0\,2$ V
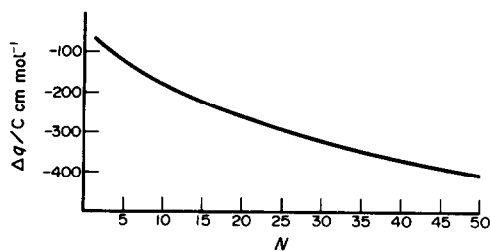

Fig 8 Plot of Δq vs the number of halfcycles for a time-symmetric square wave perturbing potential $\tau = 1$ s, $\Delta E = 0\,2$ V

5. CONCLUSIONS

The model allows to calculate the concentration profiles at any time of reactants and products for a diffusion controlled electrochemical redox reaction involving soluble species in solution under a square wave perturbing potential where only the reactant is present at the initiation of the reaction

The equations for the charge density and current density transients at each halfcycle are also obtained from the model The influence of the applied potential, duration (t') and halfperiod on the current can be evaluated A linear relationship between the current density and the reactant concentration originally present in the solution has been established

When $\tau_a/\tau_c = 1$, the current transients exhibit no substantial variation with the number of halfcycles The absolute values of the current for the anodic and cathodic halfcycles are of the same order of magnitude, despite the fact that for a constant t' value the absolute values of the current in the anodic halfcycles increase and in the cathodic halfcycles decrease according to N

Otherwise, when $\tau_a/\tau_c < 1$ the cathodic current decreases with N, and it is possible to draw a current time envelope including all halfcycles which approaches very closely the current transient predicted for a constant single potential step applied to reaction model during a time equal to the sum of τ_c for the cathodic halfcycles The better the approach the lower the τ_a/τ_c ratio

Finally, when $\tau_a/\tau_c > 1$, a fast stabilization of the current transients is observed for both anodic and cathodic halfcycles Nevertheless, it should be noticed that for $\tau_a/\tau_c > 10^3$ negative currents in the anodic halfcycles can be noticed The equations developed from the model indicate that throughout the application of square wave perturbing potential it is possible to change at will the relative rates of the anodic and cathodic reactions

REFERENCES

1 J C Canullo, W E Triaca and A J Arvia, *J electroanal Chem* **175**, 337 (1984)

2 A Visintin, J C Canullo, W E Triaca and A J Arvia, *J electroanal Chem* **239**, 67 (1988)
3 E Yeager and A J Salkind, in *Techniques of Electrochemistry*, J Wiley, New York (1973)
4 A R Despic and K I Popov, *J appl Electrochem* **1**, 275 (1971)
5 S L Marchiano, L Rebollo Neira and A J Arvia, *Electrochim Acta*, in press
6 S L Marchiano and A J Arvia, in *Comprehensive Treatise of Electrochemistry* (Edited by E Yeager, J O'M

Bockris, B E Conway and S Sarangapani), Ch 2, p 65, Plenum Press, New York (1983)
7 P Delahay, *New Instrumental Methods in Electrochemistry*, Interscience, New York, (1966)
8 C I Elsner, S L Marchiano and A J Arvia, in preparation
9 J Newman, in *Advances in Electrochemistry and Electrochemical Engineering* (Edited by P Delahay and Ch W Tobias), Vol 5, p 87, Interscience, New York (1966)